

A Robust Molecular Porous Material with High CO₂ Uptake and Selectivity

Patrick S. Nugent, Vanessah Lou Rhodus, Tony Pham, Katherine Forrest, Lukasz Wojtas, Brian Space, and Michael J. Zaworotko*

Department of Chemistry, University of South Florida, 4202 East Fowler Avenue, CHE205, Tampa, Florida 33620, United States

S Supporting Information

ABSTRACT: We report MPM-1-TIFSIX, a molecular porous material (MPM) based upon the neutral metal complex [Cu₂(adenine)₄(TiF₆)₂], that self-assembles through a hydrogen-bonding network. This MPM is amenable to room-temperature synthesis and activation. Gas adsorption measurements and ideal adsorbed solution theory selectivity predictions at 298 K revealed enhanced CO₂ separation performance relative to a previously known variant as well as the highest CO₂ uptake and isosteric heat of adsorption yet reported for an MPM. MPM-1-TIFSIX is thermally stable to 568 K and retains porosity and capacity even after immersion in water for 24 h.

Because of their extra-large surface areas and structural tunability, porous coordination polymers (PCPs)¹ and metal–organic frameworks (MOFs)² are promising candidates for gas separations,³ gas storage,⁴ heterogeneous catalysis,⁵ and sensing.⁶ Comparatively, although many molecular inclusion compounds are known,⁷ molecular solids that exhibit permanent porosity to the degree observed in PCPs are rare, presumably because molecular building blocks exhibit a tendency to pack more densely than PCPs. Therefore, the design of robust molecular porous materials (MPMs)⁸ with fine-tunable components is more challenging than in the case of PCPs. Porosity in MPMs, as defined by reversible gas adsorption, is classified as either intrinsic (inside the molecules) or extrinsic (between the molecules). Intrinsically porous MPMs are exemplified by cucurbit[*n*]urils,⁹ *tert*-butylcalix[4]-arene,¹⁰ organic cage compounds,¹¹ metal–organic squares (MOSS) and cubes (MOCs),¹² metal–organic macrocycles,¹³ and metal–organic polyhedra (MOPs).¹⁴ Cucurbit[*n*]urils, organic cage compounds, MOSS, MOCs, and MOPs possess both extrinsic and intrinsic porosity, while triptycene tris-(benzimidazolone) (TTBI),¹⁵ PUNCs,¹⁶ certain dipeptides,¹⁷ SOF-1a,¹⁸ and HOF-1¹⁹ exhibit just extrinsic porosity. TTBI presently exhibits the highest BET surface area among MPMs (2796 m²/g), but its CO₂ uptake at 273 K and 1 atm is only 81 cm³/g. While very few MPMs exhibiting surface areas above 1000 m²/g have been reported,^{11a,15,16,20} recent reports suggest that non-covalent forces,^{11a,16,21} including hydrogen bonding,^{12,15} can be utilized to rationally construct families of porous materials that are fine-tunable (i.e. platforms).

The search for porous materials is driven by the advantages that physisorption might offer over costly and energy-intensive

technologies such as amine scrubbing and cryogenic distillation.^{3b,c} A viable CO₂ capture material should exhibit high selectivity versus CH₄ and N₂ as well as thermal and water stability. We herein report a new class of MPMs in the context of physisorptive CO₂ capture through the study of an MPM platform that exhibits such features. A number of existing MPMs are known to exhibit selective CO₂ adsorption,^{9,11b,c,15,19,22} but their performance does not yet approach that of PCPs.^{3c} Specifically, the fact that inorganic anions can enhance CO₂ uptake and selectivity²³ prompted us to study the effect of axial ligand substitution in an extrinsically porous hydrogen-bonding network based upon a discrete dinuclear “paddlewheel” (PW) complex. [Cu₂(ade)₄Cl₂]Cl₂ (ade = adenine), designated MPM-1-Cl,²⁴ was thereby modified to afford [Cu₂(ade)₄(TiF₆)₂] (MPM-1-TIFSIX), a robust MPM with high CO₂ uptake and selectivity under conditions relevant to carbon capture.

We reasoned that pore functionality could be systematically varied by substituting the Cl[−] ligands lining the channels of MPM-1-Cl. We chose TiF₆^{2−} (“TIFSIX”) for this purpose, as a porous *pcu* net containing TIFSIX exhibited higher CO₂/N₂ selectivity and higher CO₂ uptake at low loading relative to variants containing SiF₆^{2−} (SIFSIX) and SnF₆^{2−} (SNIFSIX).^{23b} Accordingly, solvent diffusion of a 1:1 acetonitrile/H₂O solution of ade into an aqueous solution of Cu(NO₃)₂·2.5H₂O and (NH₄)₂TiF₆ afforded purple, rectangular prismatic single crystals of [Cu₂(ade)₄(TiF₆)₂]·2CH₃CN (MPM-1-TIFSIX) in 51% yield after 4 days [see the Supporting Information (SI)]. Single-crystal X-ray diffraction (XRD) revealed that MPM-1-TIFSIX consists of neutral PWs that crystallize in space group *R* $\bar{3}m$ with a motif very similar to that of MPM-1-Cl (Figure 1 and Table S1 in the SI).

The PW complexes in MPM-1-TIFSIX feature four bridging equatorial ade ligands and two monodentate axial TIFSIX ligands, and they self-assemble into an extrinsically porous hydrogen-bonding network. The net is reminiscent of a kagomé lattice,²⁵ and like that in MPM-1-Cl, it contains hourglass-shaped channels (~7.0 and 6.2 Å diameter in MPM-1-TIFSIX and MPM-1-Cl, respectively) and small trigonal channels that lie parallel to the *c* axis. The larger channels, which are lined with TIFSIX anions, and the small channels, which are occupied by acetonitrile molecules, are wider than those in MPM-1-Cl.

Received: June 1, 2013

Published: July 16, 2013

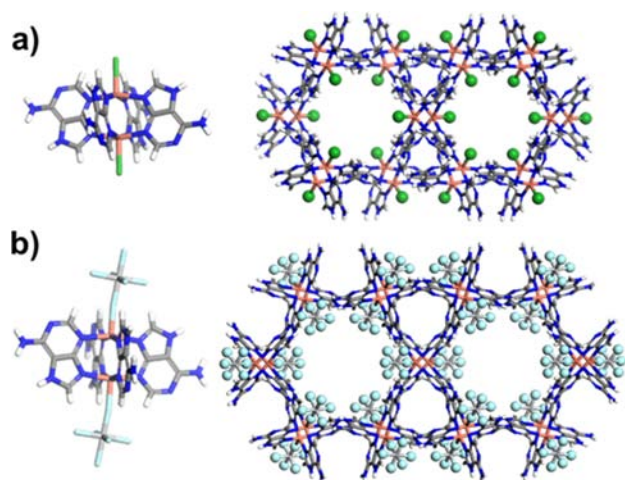


Figure 1. Views of (left) the PW complexes and (right) the networks along the *c* axis in (a) **MPM-1-Cl** and (b) **MPM-1-TIFSIX**. Solvent has been omitted for clarity. Atom colors: Cu, peach; Cl, green; Ti, silver; F, cyan; C, gray; N, blue; H, white.

The hydrogen bonding network in **MPM-1-TIFSIX** is more extensive than that in **MPM-1-Cl**. While each PW in **MPM-1-Cl** forms a total of 12 contacts (eight with its nearest neighbors and four to Cl^- counterions), each PW in **MPM-1-TIFSIX** interacts with its eight nearest neighbors via a total of 24 contacts. While the *ade-ade* contacts in **MPM-1-TIFSIX** share the same complementary motif as those in **MPM-1-Cl**, differences in the hydrogen bonding in the two networks result from the nature of the axial ligand (Figure 2). In **MPM-1-**

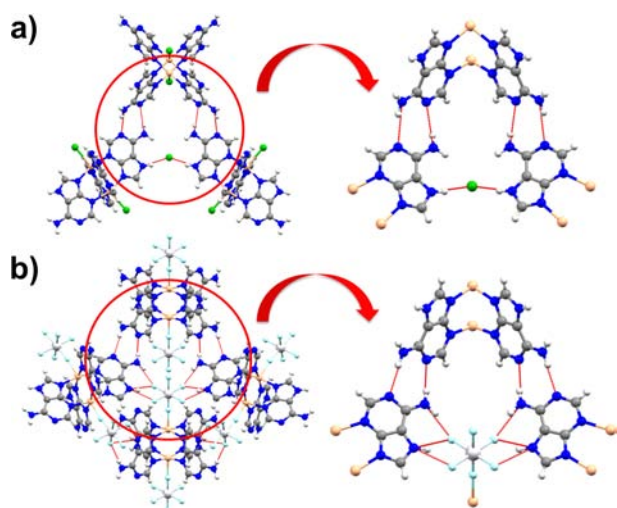


Figure 2. Hydrogen-bonding motifs in (a) **MPM-1-Cl** and (b) **MPM-1-TIFSIX**. Hydrogen bonds are shown as red dashed lines; portions of the enlarged structures at the right have been omitted for clarity.

Cl, the counterions are directly engaged in the hydrogen-bonding network and link the *ade* moieties of adjacent PWs. The axial Cl^- ligands form no contacts with other network components. In contrast, the bulkier TIFSIX ligands in **MPM-1-TIFSIX** assume a role in the network analogous to that played by the counterions in **MPM-1-Cl** (Figure 2). The $\text{F}\cdots\text{HN}$ contacts (2.73, 2.82, and 2.94 Å) in the former are shorter and more numerous than the $\text{Cl}^-\cdots\text{HN}$ contacts (3.03 Å) in the latter. The hydrogen-bond motif adopted by the

TIFSIX ligands causes the PWs to tilt 7.7° (relative to those in **MPM-1-Cl**) towards an orientation that is closer to perpendicular with the *ab* plane. This subtle change in orientation is responsible for the wider channels in **MPM-1-TIFSIX** relative to **MPM-1-Cl**.

MPM-1-Cl was synthesized according to the reported procedure²⁴ to further study its gas sorption behavior and compare it to **MPM-1-TIFSIX**. Powder X-ray diffraction (PXRD) patterns of as-synthesized **MPM-1-TIFSIX** and **MPM-1-Cl** were observed to match those calculated from single-crystal data (Figures S1 and S2 in the SI). We validated that the reported surface area of **MPM-1-Cl** measured by N_2 adsorption at 77 K is much lower than expected ($68 \text{ m}^2/\text{g}$). However, the CO_2 isotherm measured at 195 K displays reversible type-I character and reveals an experimental (calculated²⁶) Langmuir surface area of $637 (786) \text{ m}^2/\text{g}$ (Figures S3 and S4). The authors of the initial study concluded that strong interactions between N_2 and the channel windows at 77 K hinder diffusion into the material. Restricted N_2 uptake at 77 K but type-I CO_2 uptake at 195 K has been observed previously in materials with pore sizes larger than the kinetic diameter of N_2 (see the SI).²⁷ Single-gas CO_2 , CH_4 , and N_2 isotherms were collected for **MPM-1-Cl** at 298 K up to 1 atm (Figure 3). Uptakes of 44.2, 13.8, and $4.7 \text{ cm}^3/\text{g}$, respectively, at 1 atm were measured.

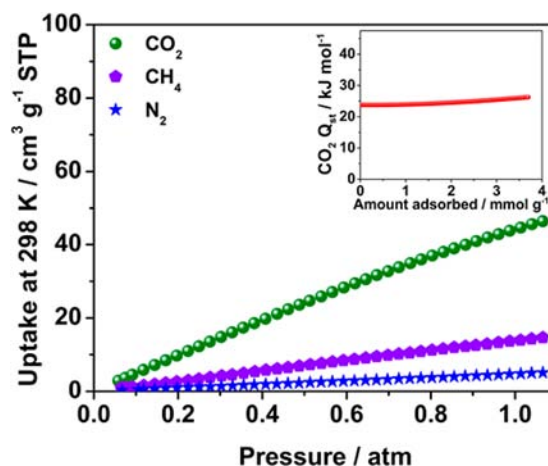


Figure 3. Low-pressure CO_2 , CH_4 , and N_2 isotherms collected at 298 K and (inset) $\text{CO}_2 Q_{\text{st}}$ for **MPM-1-Cl**.

Activation of **MPM-1-TIFSIX** at room temperature resulted in reversible type-I adsorption of CO_2 at 195 K and an experimental (calculated) BET surface area of $840 (809) \text{ m}^2/\text{g}$. The higher surface area can be attributed to the greater channel width and solvent-accessible volume of **MPM-1-TIFSIX** (49.4 vs 36.5% for **MPM-1-Cl**).²⁸ Void analysis of the desolvated form of **MPM-1-TIFSIX** using Mercury²⁹ (probe radius = 1.65 Å) revealed the existence of an accessible passage connecting the large channels that is not present in **MPM-1-Cl**. The analysis also suggested that the small channels in **MPM-1-TIFSIX** are accessible, unlike those in **MPM-1-Cl** (Figures S5–S7). The CO_2 isotherm of **MPM-1-TIFSIX** at 298 K (Figure 4) revealed much steeper adsorption at low partial pressures and 103% greater uptake at 1 atm ($89.6 \text{ cm}^3/\text{g}$) than observed for **MPM-1-Cl**. Indeed, the CO_2 uptake by **MPM-1-TIFSIX** under ambient conditions is superior to that of most PCPs and is to our knowledge the highest yet exhibited by an MPM. The CH_4

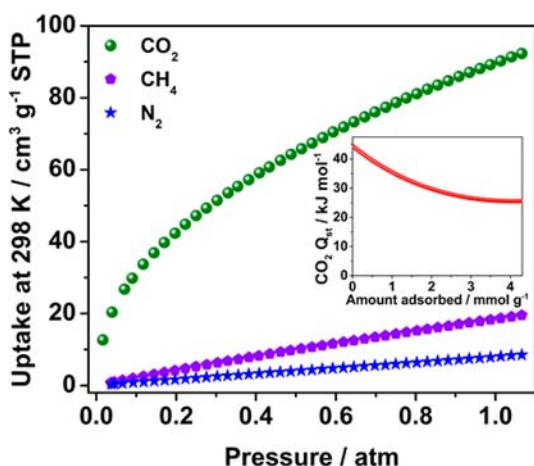


Figure 4. Low-pressure CO₂, CH₄, and N₂ isotherms collected at 298 K and (inset) CO₂ Q_{st} for MPM-1-TIFSIX.

and N₂ uptakes for MPM-1-TIFSIX at 1 atm were found to be 18.5 and 8.0 cm³/g, respectively. The shape of the CO₂ isotherm in MPM-1-TIFSIX relative to that of MPM-1-Cl suggests that the former exhibits a significantly higher isosteric heat of adsorption (Q_{st}) and selectivity toward CO₂ over CH₄ and N₂. The CO₂ Q_{st} values (Figures 3 and 4), which were calculated by fitting the 273 and 298 K isotherms to the virial equation (Figures S8 and S9), reveal that MPM-1-TIFSIX has a far higher affinity toward CO₂ at low loading (44.4 vs 23.8 kJ/mol). To our knowledge, the CO₂ Q_{st} of MPM-1-TIFSIX at zero loading is the highest yet observed among MPMs^{9,18} and is comparable to that of top-performing PCPs with saturated metal centers (SMCs) such as MOOFOR-1-Ni,^{23c} SIFSIX-3-Zn,^{23d} and UTSA-16³⁰ (Q_{st} = 56, 45, and 35 kJ/mol, respectively). Mg-dobdc, a PCP with unsaturated metal centers (UMCs), exhibits an initial Q_{st} of 47 kJ/mol.³¹

The shapes of the Q_{st} curves further suggest that MPM-1-TIFSIX possesses two or more CO₂ binding sites with different affinities whereas MPM-1-Cl is much more homogeneous in terms of binding sites. The results of grand canonical Monte Carlo (GCMC) simulations of CO₂ sorption in MPM-1-TIFSIX are in good agreement with the experimental data and further suggest the presence of multiple binding sites (Figures S10–S13 and Table S2). The primary binding site involves coordination of CO₂ to two TIFSIX anions in a confined passage connecting the large channels. Secondary binding to the TIFSIX anions lining the large channels also occurs. Charge–quadrupole interactions govern the binding at the first two sites. Lastly, sorption was observed in the small channels. These results are consistent with our assertions that inorganic anions can drive selectivity.^{23a,b,d} Because of the confined space at the primary and tertiary sites, size exclusion may also contribute to the selectivity for CO₂ over CH₄ and N₂.

To predict the CO₂ separation performance of MPM-1-TIFSIX and MPM-1-Cl at 298 K, selectivities for 10:90 CO₂/N₂ and 50:50 CO₂/CH₄ binary mixtures were calculated up to 1 atm from the pure-component isotherms via ideal adsorbed solution theory (IAST) (Table S3).³² These mixture compositions mimic those found in post-combustion capture and biogas purification, respectively. Strikingly, substitution of TIFSIX in place of Cl[−] affords 6-fold and 5-fold enhancements in the CO₂ selectivity at 1 atm (Figure 5) for the CO₂/N₂ and CO₂/CH₄ mixtures, respectively (CO₂/N₂: 74.1 vs 12.5; CO₂/CH₄: 20.3 vs 4.0). The selectivity of MPM-1-TIFSIX for CO₂

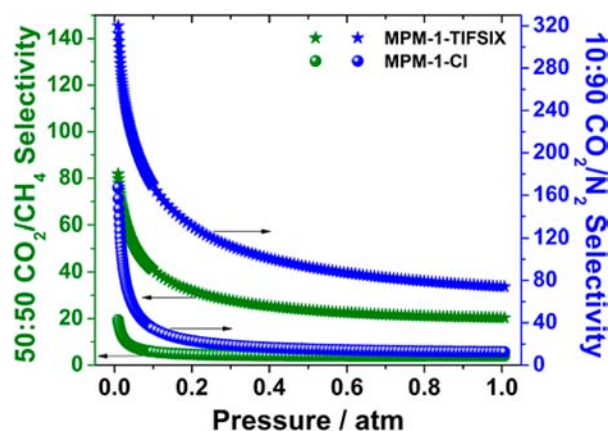


Figure 5. IAST selectivities for 50:50 CO₂/CH₄ (green; left ordinate) and 10:90 CO₂/N₂ (blue; right ordinate) binary mixtures predicted at 298 K for MPM-1-TIFSIX (★) and MPM-1-Cl (●).

over CH₄ and N₂ under these conditions is among the highest reported for MPMs and greater than those for the majority of PCPs.^{3c} Notably, many MPMs with high selectivity have significantly lower CO₂ uptake than MPM-1-TIFSIX.

In addition to selectivity, practical CO₂ separations require materials that possess thermal and water stability (flue gas is composed of ca. 6% water). MPM-1-TIFSIX was evaluated for these criteria via variable-temperature PXRD and sorption measurements (Figures S14–S16). PXRD revealed that MPM-1-TIFSIX retains its crystal structure at 568 K and after immersion in water at room temperature for 24 h (Figure S1). Sorption isotherms of activated MPM-1-TIFSIX after water exposure confirmed that the surface area and CO₂ uptake are minimally affected. By comparison, MPM-1-Cl exhibits thermal stability up to 513 K but loses its crystallinity after exposure to water for 24 h.²⁴

To conclude, through axial ligand substitution we have diversified an extrinsically porous MPM platform to include a TIFSIX-functionalized variant with SMCs that is sustained by an extensive hydrogen-bonding network. MPM-1-TIFSIX can be synthesized in a single step from commercially available starting materials and activated at room temperature. In addition to dramatically surpassing MPM-1-Cl with regard to CO₂ separation performance, MPM-1-TIFSIX exhibits the highest CO₂ uptake and Q_{st} observed in an MPM and high CO₂/N₂ and CO₂/CH₄ selectivities. MPM-1-TIFSIX also exhibits excellent thermal and water stability, which are as important as selectivity for practical applications. Further studies will be conducted on gas mixtures, and the effect of decoration with other inorganic anions (e.g., SiF₆^{2−}, SnF₆^{2−}, and ZrF₆^{2−}) on the selectivity will be addressed.

■ ASSOCIATED CONTENT

📄 Supporting Information

Crystal data (CIF); PXRD, gas sorption, and Q_{st} data; void analysis; simulations; IAST details; and structural descriptions. This material is available free of charge via the Internet at <http://pubs.acs.org>.

■ AUTHOR INFORMATION

Corresponding Author

xtal@usf.edu

Notes

The authors declare no competing financial interest.

■ ACKNOWLEDGMENTS

M.J.Z. acknowledges the U.S. Department of Energy (DE-AR0000177). B.S. acknowledges the National Science Foundation (CHE-1152362) and the computational resources made available by an XSEDE Grant (TG-DMR090028).

■ REFERENCES

- (1) (a) Kitagawa, S.; Kitaura, R.; Noro, S. *Angew. Chem., Int. Ed.* **2004**, *43*, 2334. (b) Batten, S. R.; Neville, S. M.; Turner, D. R. *Coordination Polymers: Design, Analysis and Application*; Royal Society of Chemistry: Cambridge, U.K., 2009.
- (2) (a) Eddaoudi, M.; Jaheon, K.; Rosi, N.; Vodak, D.; Wachter, J.; O'Keeffe, M.; Yaghi, O. M. *Science* **2002**, *295*, 469. (b) MacGillivray, L. R. *Metal-Organic Frameworks: Design and Application*; Wiley: Hoboken, NJ, 2010.
- (3) (a) Li, J. R.; Kuppler, R. J.; Zhou, H. C. *Chem. Soc. Rev.* **2009**, *38*, 1477. (b) D'Alessandro, D. M.; Smit, B.; Long, J. R. *Angew. Chem., Int. Ed.* **2010**, *49*, 6058. (c) Sumida, K.; Rogow, D. L.; Mason, J. A.; McDonald, T. M.; Bloch, E. D.; Herm, Z. R.; Bae, T. H.; Long, J. R. *Chem. Rev.* **2012**, *112*, 724.
- (4) Murray, L. J.; Dincă, M.; Long, J. R. *Chem. Soc. Rev.* **2009**, *38*, 1294.
- (5) Ma, L.; Abney, C.; Lin, W. *Chem. Soc. Rev.* **2009**, *38*, 1248.
- (6) Halder, G. J.; Kepert, C. J.; Moubaraki, B.; Murray, K. S.; Cashion, J. D. *Science* **2002**, *298*, 1762.
- (7) (a) Barrer, R. M.; Shanson, V. H. *J. Chem. Soc., Chem. Commun.* **1976**, 333. (b) Endo, K.; Sawaki, T.; Koyanagi, M.; Kobayashi, K.; Masuda, H.; Aoyama, Y. *J. Am. Chem. Soc.* **1995**, *117*, 8341. (c) Allison, S. A.; Barrer, R. M. *J. Chem. Soc. A* **1969**, 1717.
- (8) (a) McKeown, N. B. *J. Mater. Chem.* **2010**, *20*, 10588. (b) Tian, J.; Thallapally, P. K.; McGrail, B. P. *CrystEngComm* **2012**, *14*, 1909.
- (9) (a) Kim, H.; Kim, Y.; Yoon, M.; Lim, S.; Park, S. M.; Seo, G.; Kim, K. *J. Am. Chem. Soc.* **2010**, *132*, 12200. (b) Tian, J.; Ma, S.; Thallapally, P. K.; Fowler, D.; McGrail, B. P.; Atwood, J. L. *Chem. Commun.* **2011**, 47, 7626.
- (10) Atwood, J. L.; Barbour, L. J.; Jerga, A. *Angew. Chem., Int. Ed.* **2004**, *43*, 2948.
- (11) (a) Jones, J. T. A.; Hasell, T.; Wu, X.; Bacsa, J.; Jelfs, K. E.; Schmidtman, M.; Chong, S. Y.; Adams, D. J.; Trewin, A.; Schiffrman, F.; Cora, F.; Slater, B.; Steiner, A.; Day, G. M.; Cooper, A. I. *Nature* **2011**, *474*, 367. (b) Mastalerz, M.; Schneider, M. W.; Opperl, I. M.; Presly, O. *Angew. Chem., Int. Ed.* **2011**, *50*, 1046. (c) Jin, Y.; Voss, B. A.; Jin, A.; Long, H.; Noble, R. D.; Zhang, W. *J. Am. Chem. Soc.* **2011**, *133*, 6650.
- (12) (a) Wang, S.; Zhao, T.; Li, G.; Wojtas, L.; Huo, Q.; Eddaoudi, M.; Liu, Y. *J. Am. Chem. Soc.* **2010**, *132*, 18038. (b) Sava, D. F.; Kravtsov, V. C.; Eckert, J.; Eubank, J. F.; Nouar, F.; Eddaoudi, M. *J. Am. Chem. Soc.* **2009**, *131*, 10394.
- (13) An, J.; Fiorella, R. P.; Geib, S. J.; Rosi, N. L. *J. Am. Chem. Soc.* **2009**, *131*, 8401.
- (14) Ni, Z.; Yassar, A.; Antoun, T.; Yaghi, O. M. *J. Am. Chem. Soc.* **2005**, *127*, 12752.
- (15) Mastalerz, M.; Opperl, I. M. *Angew. Chem., Int. Ed.* **2012**, *51*, 5252.
- (16) Bezzu, C. G.; Helliwell, M.; Warren, J. E.; Allan, D. R.; McKeown, N. B. *Science* **2010**, *327*, 1627.
- (17) (a) Gorbitz, C. *Acta Crystallogr.* **2002**, *B58*, 849. (b) Gorbitz, C. H.; Gundersen, E. *Acta Crystallogr.* **1996**, *C52*, 1764.
- (18) Yang, W.; Greenaway, A.; Lin, X.; Matsuda, R.; Blake, A. J.; Wilson, C.; Lewis, W.; Hubberstey, P.; Kitagawa, S.; Champness, N. R.; Schröder, M. *J. Am. Chem. Soc.* **2010**, *132*, 14457.
- (19) He, Y.; Xiang, S.; Chen, B. *J. Am. Chem. Soc.* **2011**, *133*, 14570.
- (20) Schneider, M. W.; Opperl, I. M.; Ott, H.; Lechner, L. G.; Hauswald, H.-J. S.; Stoll, R.; Mastalerz, M. *Chem.—Eur. J.* **2012**, *18*, 836.
- (21) Bojdys, M. J.; Briggs, M. E.; Jones, J. T. A.; Adams, D. J.; Chong, S. Y.; Schmidtman, M.; Cooper, A. I. *J. Am. Chem. Soc.* **2011**, *133*, 16566.
- (22) (a) Tian, J.; Liu, J.; Liu, J.; Thallapally, P. K. *CrystEngComm* **2013**, *15*, 1528. (b) Comotti, A.; Bracco, S.; Distefano, G.; Sozzani, P. *Chem. Commun.* **2009**, 284.
- (23) (a) Burd, S. D.; Ma, S.; Perman, J. A.; Sikora, B. J.; Snurr, R. Q.; Thallapally, P. K.; Tian, J.; Wojtas, L.; Zaworotko, M. J. *J. Am. Chem. Soc.* **2012**, *134*, 3663. (b) Nugent, P.; Rhodus, V.; Pham, T.; Tudor, B.; Forrest, K.; Wojtas, L.; Space, B.; Zaworotko, M. *Chem. Commun.* **2013**, 49, 1606. (c) Mohamed, M. H.; Elsaïdi, S. K.; Wojtas, L.; Pham, T.; Forrest, K. A.; Tudor, B.; Space, B.; Zaworotko, M. J. *J. Am. Chem. Soc.* **2012**, *134*, 19556. (d) Nugent, P.; Belmabkhout, Y.; Burd, S. D.; Cairns, A. J.; Luebke, R.; Forrest, K.; Pham, T.; Ma, S.; Space, B.; Wojtas, L.; Eddaoudi, M.; Zaworotko, M. J. *Nature* **2013**, *495*, 80.
- (24) Thomas-Gipson, J.; Beobide, G.; Castillo, O.; Cepeda, J.; Luque, A.; Perez-Yanez, S.; Aguayo, A. T.; Roman, P. *CrystEngComm* **2011**, *13*, 3301.
- (25) Moulton, B.; Lu, J.; Hajndl, R.; Hariharan, S.; Zaworotko, M. J. *Angew. Chem., Int. Ed.* **2002**, *41*, 2821.
- (26) Düren, T.; Millange, F.; Férey, G.; Walton, K. S.; Snurr, R. Q. *J. Phys. Chem. C* **2007**, *111*, 15350.
- (27) (a) Ok, K. M.; Sung, J.; Hu, G.; Jacobs, R. M. J.; O'Hare, D. J. *J. Am. Chem. Soc.* **2008**, *130*, 3762. (b) Maji, T. K.; Matsuda, R.; Kitagawa, S. *Nat. Mater.* **2007**, *6*, 142. (c) Jiang, J. J.; Pan, M.; Liu, J. M.; Wang, W.; Su, C. Y. *Inorg. Chem.* **2010**, *49*, 10166.
- (28) Spek, A. L. *J. Appl. Crystallogr.* **2003**, *36*, 7.
- (29) Bruno, I. J.; Cole, J. C.; Edgington, P. R.; Kessler, M.; Macrae, C. F.; McCabe, P.; Pearson, J.; Taylor, R. *Acta Crystallogr.* **2002**, *B58*, 389.
- (30) Xiang, S.; He, Y.; Zhang, Z.; Wu, H.; Zhou, W.; Krishna, R.; Chen, B. *Nat. Commun.* **2012**, *3*, 954.
- (31) Caskey, S. R.; Wong-Foy, A. G.; Matzger, A. J. *J. Am. Chem. Soc.* **2008**, *130*, 10870.
- (32) (a) Myers, A. L.; Prausnitz, J. M. *AIChE J.* **1965**, *11*, 121. (b) Bae, Y. S.; Mulfort, K. L.; Frost, H.; Ryan, P.; Punnathanam, S.; Broadbelt, L. J.; Hupp, J. T.; Snurr, R. Q. *Langmuir* **2008**, *24*, 8592.